

Journal of Mechanics of Materials and Structures

**MEASUREMENT OF ELASTIC PROPERTIES OF AISI 52100
ALLOY STEEL BY ULTRASONIC NONDESTRUCTIVE METHODS**

Mohammad Hamidnia and Farhang Honarvar

Volume 7, No. 10

December 2012



MEASUREMENT OF ELASTIC PROPERTIES OF AISI 52100 ALLOY STEEL BY ULTRASONIC NONDESTRUCTIVE METHODS

MOHAMMAD HAMIDNIA AND FARHANG HONARVAR

In certain applications, it is important to measure the mechanical properties of steel with high accuracy. These measurements are usually performed by destructive processes, in which the test sample is destroyed. Destructive techniques cannot detect the minuscule changes made in the mechanical properties of steel during heat treatment processes. Ultrasonic nondestructive testing is an alternative method that can be used for measuring the mechanical properties of steel more precisely. In this paper, the ultrasonic method is used for measuring the elastic properties of AISI 52100 steel samples which are heat treated at different levels. Each sample has its specific microstructure and hardness due to the heat treatment process it has gone through. The elastic properties of each sample are obtained by measuring the velocities of longitudinal and shear waves in each sample. Comparison of the results obtained from ultrasonic measurements with those available in reference tables shows that the ultrasonic technique can measure the elastic properties of AISI 52100 samples with high accuracy. The ultrasonic technique also shows that it can identify the tempered martensite embrittlement zone in AISI 52100 samples.

1. Introduction

Most mechanical parts used in industrial applications are subjected to some sort of heat treatment. It is essential to verify if the heat-treatment process is done properly and if the component has acquired the desired properties after processing [Badidi Bouda et al. 2000]. Destructive techniques, which are based on variations of physical and mechanical properties of the material, cannot clearly distinguish the slight differences in the microstructure of the material [Vasudevan and Palanichamy 2002]. However, the study of ultrasonic wave propagation in metals and composites can provide information on the microstructure as well as the mechanical and physical properties of the material. The changes made in the atomic structure of materials during a heat-treatment process have been studied before [Ringer et al. 1997] but in this work, we only consider the overall changes observed in the ultrasonic and mechanical properties of the material. Ultrasonic techniques are used not only to detect discontinuities, such as voids, cracks, and inclusions, but also to evaluate such material characteristics as microstructure, grain size, yield strength, fracture toughness, volume fraction of second phase, and residual stress [Kumar et al. 2003]. Quantitative assessment of microstructural changes and mechanical properties can be carried out by measuring ultrasonic parameters such as wave velocity and attenuation [Birks et al. 1991]. The ultrasonic wave velocity depends on elastic constants and density of the body while the attenuation depends on microstructure and crystalline defects [Rokhlin and Matikas 1996; Carreon et al. 2009].

The relationship between ultrasonic and mechanical properties has been studied for various materials, including tempered CA-15 martensitic stainless steel [Hsu et al. 2004], SiC ceramics [ASTM E664-93

Keywords: elastic properties, ultrasonic nondestructive method, AISI 52100 steel, heat treatment.

2000], and Nimonic alloys [Murthy et al. 2008; 2009]. A few studies have also been conducted on the dependency of ultrasonic wave velocity and microstructure of materials. Some of the materials considered for this purpose are: low-alloy steels [ASTM E92-82 2003], austenitic stainless steels [Vasudevan and Palanichamy 2002; Hakan Gür and Orkun Tuncer 2005], AISI 4140 and 5140 steels, SAE 1040 and 4140 steels [Hakan Gür and Çam 2007], alumina–zirconia ceramics [Rokhlin and Matikas 1996], and aluminum alloy 2024 [Rosen et al. 1985]. The wave velocity and attenuation of SAE 52100 samples quenched at different temperatures have also been studied by Papadakis [1970].

In this paper, we are interested in evaluating the potential of the ultrasonic nondestructive evaluation technique in the measurement of the elastic constants of AISI 52100 alloy steel samples which are hardened to different levels. Because this alloy has enormous industrial applications, the right choice of heat treatment can result in the most appropriate mechanical properties. Our purpose is to demonstrate that small changes in the mechanical properties of samples can be measured by ultrasonic testing. Any other alloy could also be used for this purpose. A number of samples are prepared and processed by different heat treatment schemes. The heat treatment processes are defined based on reference handbooks and advice from industrial experts. Ultrasonic velocity and attenuation measurements have been used to accurately measure the elastic constants, such as the Young's modulus and Poisson's ratio, of these samples in order to differentiate them from the raw sample and from one another.

2. Experiments

Preparation of specimens. The chemical composition of the AISI 52100 alloy steel (DIN 100Cr6 or DIN 1.3505/Ball and Roller bearing steels) used in the present study is given in Table 1. Six cylindrical coupon specimens, 30 mm in diameter and 6 mm in thickness, were prepared from a bar stock of AISI 52100 alloy steel. In order to compare the ultrasonic characteristics and elastic properties of these specimens, they were prepared with dimensions as similar as possible [ASTM E664-93 2000]. The test surfaces of all specimens were finished with a parallelism tolerance of 0.2 mm.

Heat treatment. From the six specimens, one (sample 1) was intact and the remaining five (2–6) were subjected to different heat treatment processes. The details of the heat treatment processes conducted on specimens 2–6 are schematically shown in Figure 1.

All five specimens were first subjected to stress-relief heat treatment in two stages. The temperatures and holding times of these two stress-relief heat treatment stages are shown in Figure 1. After the stress-relief process, all specimens were austenitized to produce austenite with a homogeneous composition of carbon and other alloying elements. The two main factors in austenitization are the temperature and the time, which were selected by the aid of a temperature-time-transformation diagram and experience [Verhoeven 2005].

All specimens were heated to 850 °C at a heating rate of 50 °C/hour and held at this temperature for 30 minutes. They were then quenched in salt bath furnaces to arrive at a temperature of 180 °C. Good heat transfer and natural convection in the salt bath furnaces was used to promote uniformity of specimen

$$\text{C} = 1\% \quad \text{Si} = 0.25\% \quad \text{Mn} = 0.35\% \quad \text{Cr} = 1.5\% \quad \text{P} = 0.015\%$$

Table 1. Chemical composition of AISI 52100 by weight.

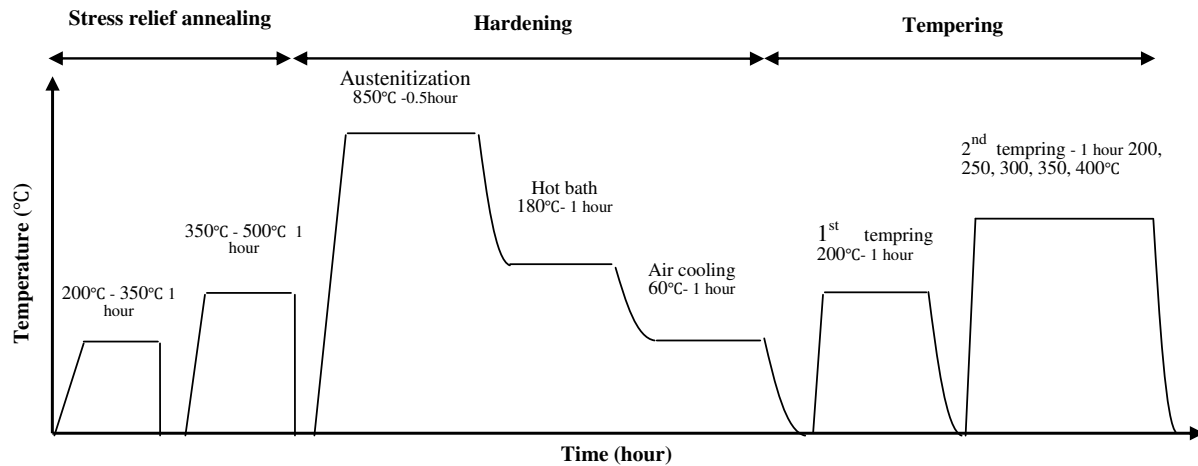


Figure 1. Heat treatment processes.

temperatures [ASM 4 1991]. The specimens were then cooled in air to arrive at 60 °C. Cooling in air at a moderate rate is to prevent large differences in temperature between the outside surface and the center core. All specimens were tempered in two stages: first, all specimens were reheated up to 200 °C for 1 hour, and second, specimens 1–5 were reheated at temperatures of 200 °C, 250 °C, 300 °C, 350 °C, and 400 °C for 1 hour, respectively. The temperature uncertainty of the oven was ± 20 °C. Tempering was accomplished by soaking the entire specimen in the furnace for enough time to bring the tempering mechanism to the desired point of completion.

The mechanical properties of tempered steel are affected by a number of variables, including: tempering temperature, duration of tempering, cooling rate from the tempering temperature, and composition of the steel [ASM 4 1991]. In order to investigate the effect of tempering temperature on the ultrasonic and mechanical properties of the specimens, the duration of tempering, cooling rate, and composition of the material were held constant and all other parameters in the stress relief annealing and hardening process were kept as identical as possible.

Hardness measurement. Hardness levels of the specimens were obtained by a Vickers hardness tester using a 10 kg load. A small indentation in the polished surface of each specimen was made using a standard procedure. For each specimen, at least five indentations were made under similar conditions and the average of the diagonal lengths of the indentations were used to compute the Vickers hardness number using the following equation [ASTM E92-82 2003]:

$$VHN = \frac{1.854}{d^2} F \quad (1)$$

where d is the diagonal length of the indentation in mm and F is the applied load in kg. The accuracy in measuring d was estimated to be $\pm 2 \mu\text{m}$.

Density measurements. Density was measured using Archimedes' principle:

$$\rho = \frac{W_a}{W_a - W_b} \rho_b, \quad (2)$$

where W_a and W_b are the weights of the specimen in air and water, respectively, and ρ_b is the density of water. All weight measurements were made using a digital weighing scale. The uncertainty in these measurements was ± 0.1 mg. The experiments were repeated five times for each specimen in order to obtain a reliable density value.

Ultrasonic velocity measurements. Figure 2 shows the configuration of the experimental setup for the contact and immersion ultrasonic testing methods. A pulser/receiver (Panametrics 5072PR), a 100 MHz A/D converter (CompuScope14100) with 14-bit resolution and a PC were employed for recording ultrasonic signals.

Ultrasonic wave velocity measurements were carried out for both longitudinal and transverse waves. The longitudinal wave velocity was measured by a 0.25 inch diameter, 10 MHz immersion focused probe (Panametrics V312-N-SU) and shear wave velocity was measured by a 0.5 inch diameter, 5 MHz contact probe (Panametrics V155). Honey was used for coupling the normal beam shear wave probe to the specimens. The time of flight of the longitudinal and transverse waves in each specimen was measured between the second and third backwall echoes. The ultrasonic wave velocity (V) was determined using the following equation [ASTM E494-95 1995]:

$$V = \frac{k \times 2d}{t_m - t_n}, \quad (3)$$

where d is the specimen thickness, k is the difference between the echo indices m and n , and t_m and t_n are the transit times of the m -th and n -th echoes, respectively. Figure 3 shows typical specimen time traces of the longitudinal and transverse waves. In the top graph, the backwall echoes of the longitudinal wave probe are not very strong and this is because the normal beam probe is a focused transducer. Due to its smaller wavelength, the shear wave is more sensitive to changes in microstructure [Palanichamy et al. 1995; Murthy et al. 2009].

Variations in ultrasonic wave velocity due to changes in material characteristics and microstructure (except changes in texture) are usually small, and therefore accurate velocity measurements are required for detecting these changes.

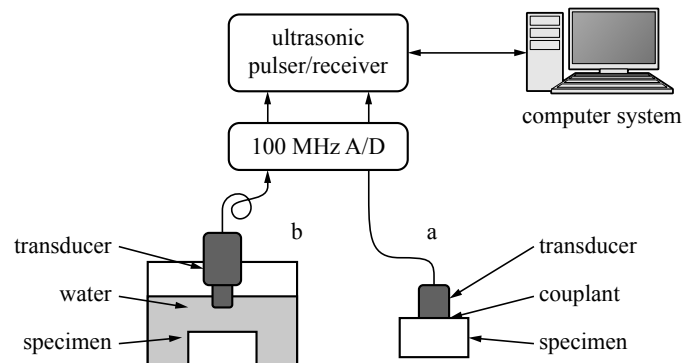


Figure 2. Schematic of the experimental setup: (a) contact method and (b) immersion method.

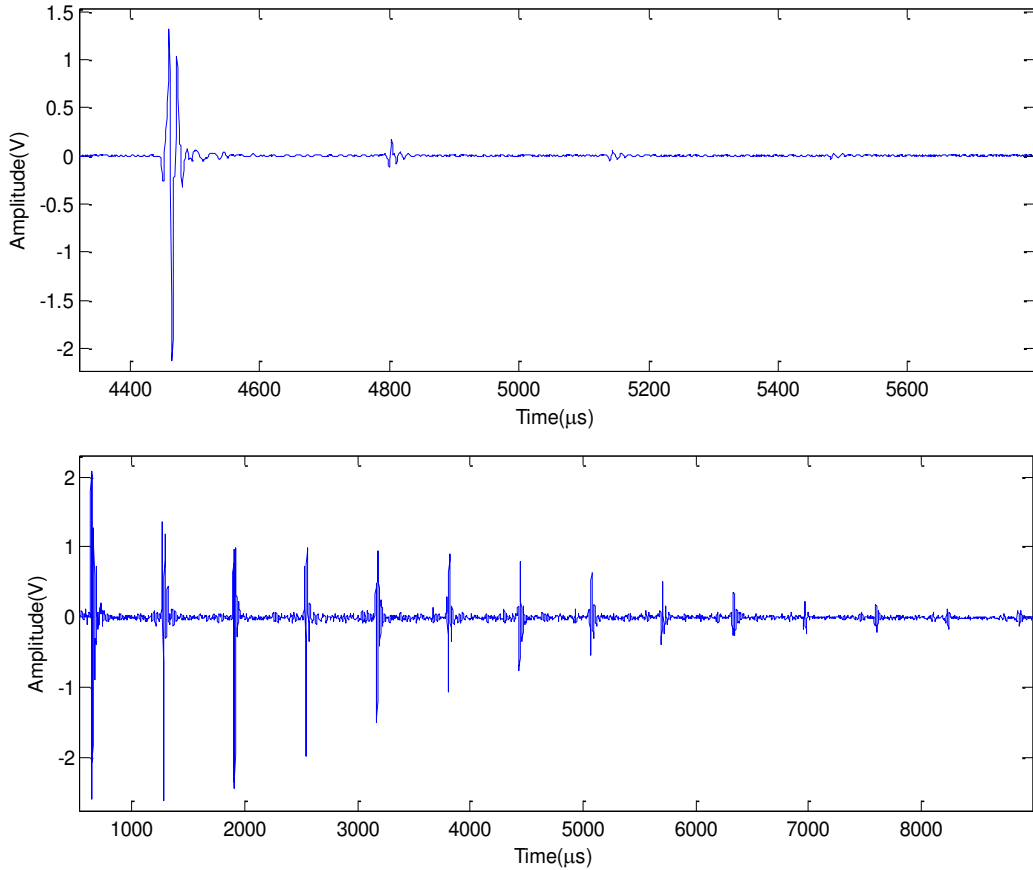


Figure 3. Specimen time traces for longitudinal (top) and transverse (bottom) waves.

The time delay between two consecutive echoes can be measured by three different time-delay measurement techniques: phase-slope, overlap, and cross-correlation [dos Santos Mesquita and Halldórsdóttir 2005]. Among these three techniques, the cross-correlation technique does not require explicit criteria for accepting or rejecting specific features in echoes affected by distortion or low signal-to-noise ratio. Therefore, in this study, the cross-correlation method is used in order to eliminate the need for the somewhat arbitrary criteria required for the other two techniques. Cross-correlation can be performed between two time signals, $x(t)$ and $y(t)$, using computer algorithms which implement the cross-correlation function $R_{xy}(t)$, defined as [Hull et al. 1985]:

$$R_{xy}(t) = \lim_{T \rightarrow \infty} \frac{1}{T} \int_0^T x(\tau)y(t + \tau) d(\tau), \quad (4)$$

where t is the time index of signals x and y , and τ is the time delay of associated components.

Ultrasonic attenuation measurements. Measurement of attenuation coefficients in materials is useful in applications such as comparison of heat treatments of different lots of material or assessment of environmental degradation of materials [Birks et al. 1991]. The attenuation coefficient of the ultrasonic wave is affected by absorption and scattering. Absorption can be due to dislocation damping, magnetic

resistance, or thermal elasticity, and scattering can be due to grain boundaries, voids, inclusions, second-phase particles, and cracks [Hsu et al. 2004].

The ultrasonic attenuation coefficient (α) is calculated from the equation

$$\alpha \text{ (dB/mm)} = \frac{20 \log A_1/A_2}{2T} \quad (5)$$

(see [ASTM E664-93 2000]), where A_1 and A_2 are peak amplitudes of the first and second transmitted echoes, and T is the test specimen thickness in millimeters.

Determination of elastic properties. Elastic properties are determined by the aggregate response of the interatomic forces among all atoms of the metal. Therefore, the presence of small quantities of solute atoms in dilute alloys or their rearrangement by heat treatment will have relatively little effect on the absolute values of elastic constants [Brandes and Brook 1998]. The determination of longitudinal and transverse wave velocities in an isotropic material makes it possible to approximately calculate the elastic constants using the following formulae [Birks et al. 1991; ASTM E494-95 1995]:

$$\sigma = \frac{1 - 2(V_s/V_l)^2}{2(1 - (V_s/V_l)^2)}, \quad E = \frac{\rho V_s(3V_l^2 - 4V_s^2)}{V_l^2 - V_s^2}, \quad G = \rho V_s^2, \quad K = \rho(V_l^2 - \frac{4}{3}V_s^2),$$

where σ is the Poisson's ratio and E , G , and K , are the Young's, shear, and bulk moduli, respectively. V_l and V_s are the ultrasonic longitudinal and transverse wave velocities, respectively. The above equations are usually used for material characterization by ultrasonic wave velocity measurements as well as for studying the effect of metallurgical parameters such as precipitation on metals in isotropic materials [ASTM E92-82 2003].

3. Results and discussion

Ultrasonic characteristics and elastic properties of the specimens were found by using the equations above. The corresponding values for the six AISI 52100 alloy steel specimens are listed in Tables 2 and 3.

Figure 4 shows the effect of tempering temperature on hardness. During tempering, martensite decomposes into a mixture of ferrite and cementite leading to a decrease in volume as tempering temperature increases. Percentage of martensitic structure as well as hardness decrease with an increase in tempering temperature. All tempered specimens had hardness values greater than the untreated specimen.

Sample	Density (kg/m ³)	Longitudinal velocity (m/s)	Transverse velocity (m/s)	Attenuation (dB/mm)	Z (kg/m ³ ·s)
1	7322	5845.2	3182.5	0.124	42798.98
2	7289	6066.9	3225.5	0.155	44221.64
3	7280	5910.4	3210.4	0.133	43024.94
4	7374	5918.3	3222.2	0.054	43644.04
5	7356	5931.4	3224.2	0.182	43634.42
6	7346	5986.6	3281.4	0.206	43978.67

Table 2. Ultrasonic characteristics of the specimens. Sample 6 was untreated. (Z is the acoustic impedance.)

Sample	Vickers hardness	Poisson's ratio	Young's modulus (GPa)	Shear modulus (GPa)	Bulk modulus (GPa)
1	849.1	0.289	191.23	74.16	151.29
2	715.6	0.303	197.61	75.83	167.18
3	692.1	0.291	193.67	75.02	154.26
4	631.4	0.289	197.43	76.56	156.21
5	579.4	0.290	197.35	76.47	156.84
6	275.3	0.285	203.33	79.10	157.81

Table 3. Elastic properties of specimens. Sample 6 was untreated.

The first two parts of Figure 5 show the effect of tempering temperature on longitudinal and transverse wave velocities. Transverse and longitudinal wave velocities increase continuously as the tempering temperature increases, except in the tempered martensite embrittlement (TME) range (260–370 °C or 500–700 °F). The TME range is also known as 500 °F embrittlement or one-step temper embrittlement [Verhoeven 2005]. Both transverse and longitudinal wave velocities show sudden increases in the TME range.

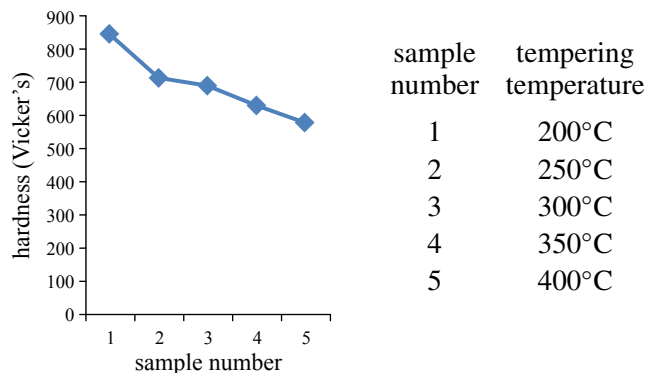


Figure 4. Effect of tempering temperature on hardness.

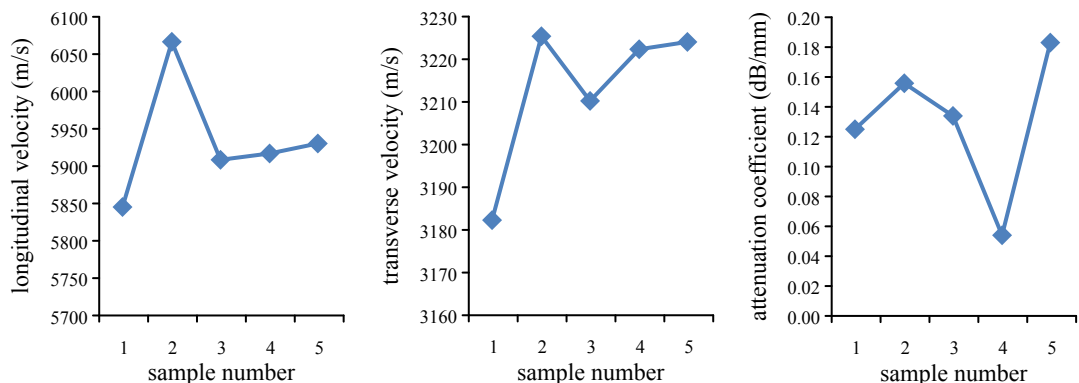


Figure 5. Effect of tempering temperature on ultrasonic properties. From left to right, longitudinal wave velocity, transverse wave velocity, and attenuation coefficient.

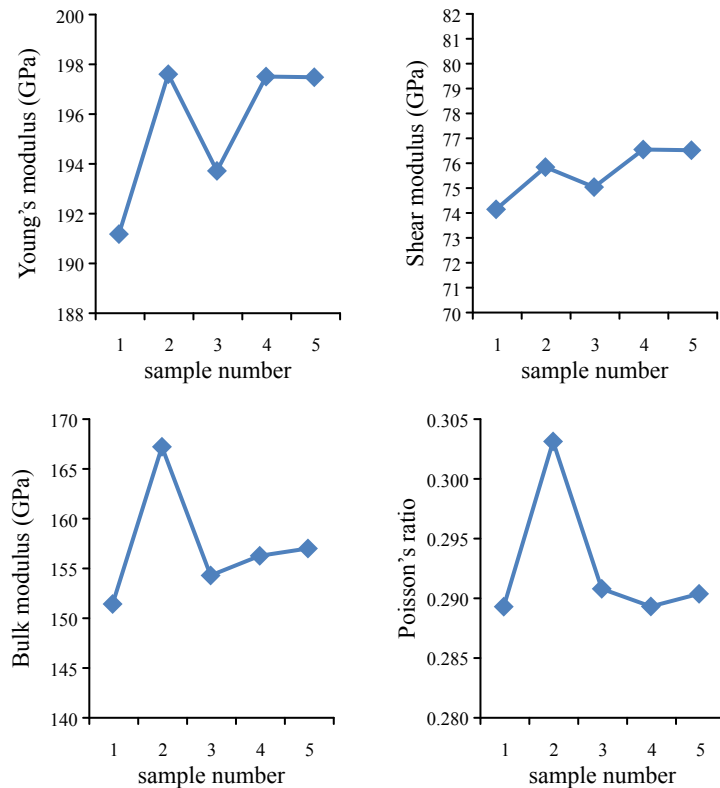


Figure 6. Effect of tempering temperature on elastic constants. Top: Young's modulus and shear modulus. Bottom: bulk modulus and Poisson's ratio.

Figure 5, right, shows the effect of tempering temperature on the attenuation of ultrasonic waves. It is observed that the attenuation data is quite scattered and no particular relationship can be established between the wave attenuation and tempering temperature. The attenuation coefficient is controlled by two phenomena: scattering and absorption. The existence of transition carbide, low-carbon martensite, and dislocations in the range 200–250 °C increase the scattering attenuation. In the temperature range 250–350 °C, cementite and ferrite appear and replace the aforementioned components which leads to a drop in the attenuation factor. Beyond the tempering temperature of 350 °C, the grain size increases and consequently the scattering attenuation also increases.

Figure 6 shows the effect of tempering temperature on elastic properties. The changes in the values of the Young's, shear, and bulk moduli with changes in tempering temperature are similar. They all increase with increase of the tempering temperature. Figure 6d shows the effect of tempering temperature on the Poisson's ratio. In Figure 6d, the Poisson's ratios of the tempered samples are approximately constant except in the TME range (also see Table 3).

Comparing Figures 4, 5 and 6, it can be observed that by increasing the tempering temperature, hardness decreases while elastic constants (the Young's, shear, and bulk moduli) and ultrasonic properties (longitudinal and transverse wave velocities and attenuation) increase except in the TME range, where the process is reversed. The major effect of tempering is elimination of many of the smaller laths and

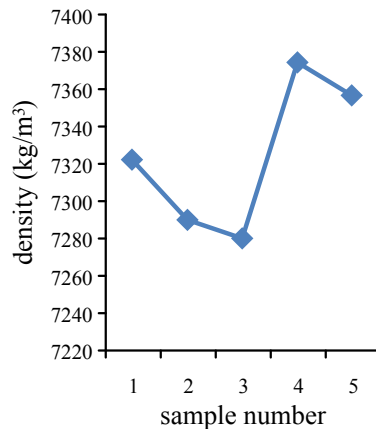


Figure 7. Effect of tempering temperature on density.

production of coarse, spherical cementite particles at the prior austenite grain boundaries and within packets [Krauss 1989]. During tempering, decomposition of martensite into ferrite and carbides creates both structural and dimensional changes. In the temperature range of 100–250 °C, transition carbide, epsilon carbide, and eta carbide form and the carbon content of matrix martensite decreases to about 0.25%. Consequently, the bct structure in the equilibrium structure of martensite tends to transform into a bcc structure.

Figure 7 shows the effect of tempering temperature on density. Because of the existence of martensite and dislocations in this range, the volume of specimens is increased and density is decreased. By increasing the tempering temperature, dislocation density is effectively lowered and any residual dislocations within laths rearrange themselves into low-angle boundaries within the equiaxed grains.

In the temperature range of 200–300 °C, the retained austenite transforms to ferrite and cementite. In plain carbon steels and low-alloy steels, the retained austenite transforms to bainite with an increase in volume and a decrease in density. By eliminating the retained austenite, volume decreases and density increases.

In the temperature range of 250–350 °C, the transition carbide and low-carbon martensite are replaced by cementite and ferrite [Krauss 1989].

It has already been shown that the formation of ferrite, coarse pearlite, fine pearlite, cementite, bainite, and martensite phases in some steels (medium-carbon low alloy steels [Krauss 1989], AISI 4140 [Palanichamy et al. 1995], 38 NiCr Mo4 [ASTM E494-95 1995]) is continuously associated with an increase in hardness and a decrease in ultrasonic velocity.

Our results show that there are more than one microstructure in each specimen and by increasing the tempering temperature, the percentage of cementite and ferrite in microstructure increases and leads to improvement in the ultrasonic and elastic properties of the tempered specimens. The abnormal behavior of mechanical and ultrasonic properties in the TME range can be due to different factors, some of the most important of which are [ASM 1 1990]:

- (1) Initiation of cementite precipitation at TME range. Low-temperature precipitated cementite is long and plate-like and is formed at grain boundaries.

- (2) Impurity elements, chiefly phosphorus, which segregate to the prior austenite grain boundaries during austenitization.
- (3) The presence of small amounts of retained austenite films between the laths of martensite.
- (4) Decomposition of interlath-retained austenite to interlath cementite.

Conclusions

The purpose of this research was to derive relationships between tempering temperature and the ultrasonic and elastic properties of AISI 52100 alloy steel. The elastic properties were obtained by measuring the longitudinal and transverse wave velocities of heat-treated AISI 52100 samples. The results show that the ultrasonic technique can identify any slight changes in the microstructure and mechanical properties of AISI 52100 alloy steel. Accordingly, one can choose the most suitable tempering temperature range for manufacturing components with specific elastic properties.

The abnormal behavior of the mechanical and ultrasonic properties of AISI 52100 alloy steel at the tempered martensite embrittlement range was noticed and possible reasons for this kind of behavior were suggested. As a future task, this behavior could be studied more precisely.

References

- [ASM 1 1990] *Properties and selection: irons, steels, and high performance alloys*, ASM Handbook **1**, ASM International, Materials Park, OH, 1990.
- [ASM 4 1991] *Heat treating*, ASM Handbook **4**, ASM International, Materials Park, OH, 1991.
- [ASTM E494-95 1995] “Standard practice for measuring ultrasonic velocity in materials”, ASTM Standard E494-95, ASTM International, 1995, Available at <http://tinyurl.com/astm-E494-95>. Replaced by E494 - 10.
- [ASTM E664-93 2000] “Standard practice for the measurement of the apparent attenuation of longitudinal ultrasonic waves by immersion method”, ASTM Standard E664-93, ASTM International, 2000, Available at <http://tinyurl.com/agbehwf>. Superseded by E664M - 10.
- [ASTM E92-82 2003] “Standard test method for Vickers hardness of metallic materials”, ASTM Standard E92-82, ASTM International, 2003, Available at <http://tinyurl.com/astm-E92-82>. Replaced by E384 - 11e1, Standard test for Knoop and Vickers hardness of materials.
- [Badidi Bouda et al. 2000] A. Badidi Bouda, A. Benchaala, and K. Alem, “Ultrasonic characterization of materials hardness”, *Ultrasonics* **38**:1–8 (2000), 224–227.
- [Birks et al. 1991] A. S. Birks, R. E. Green, Jr., and P. McIntire (editors), *Ultrasonic testing*, 2nd ed., Nondestructive Testing Handbook **7**, American Society for Nondestructive Testing, Columbus, OH, 1991.
- [Brandes and Brook 1998] E. A. Brandes and G. B. Brook (editors), *Smithells metals reference book*, 7th ed., Butterworth-Heinemann, Oxford, 1998.
- [Carreon et al. 2009] H. Carreon, A. Ruiz, A. Medina, G. Barrera, and J. Zarate, “Characterization of the alumina-zirconia ceramic system by ultrasonic velocity measurements”, *Mater. Charact.* **60**:8 (2009), 875–881.
- [Hakan Gür and Çam 2007] C. Hakan Gür and I. Çam, “Comparison of magnetic Barkhausen noise and ultrasonic velocity measurements for microstructure evaluation of SAE 1040 and SAE 4140 steels”, *Mater. Charact.* **58**:5 (2007), 447–454.
- [Hakan Gür and Orkun Tuncer 2005] C. Hakan Gür and B. Orkun Tuncer, “Characterization of microstructural phases of steels by sound velocity measurement”, *Mater. Charact.* **55**:2 (2005), 160–166.
- [Hsu et al. 2004] C.-H. Hsu, H.-Y. Teng, and Y.-J. Chen, “Relationship between ultrasonic characteristics and mechanical properties of tempered martensitic stainless steel”, *J. Mater. Eng. Perform.* **13**:5 (2004), 593–598.
- [Hull et al. 1985] D. R. Hull, H. E. Kautz, and A. Vary, “Ultrasonic velocity measurement using phase-slope and cross-correlation methods”, *Mater. Eval.* **43** (1985), 1455–1460. NASA Technical Memo 83794.

- [Krauss 1989] G. Krauss, *Steels: heat treatment and processing principles*, ASM International, Materials Park, OH, 1989.
- [Kumar et al. 2003] A. Kumar, T. Jayakumar, B. Raj, and K. K. Ray, “Characterization of solutionizing behavior in VT14 titanium alloy using ultrasonic velocity and attenuation measurements”, *Mater. Sci. Eng. A* **360**:1–2 (2003), 58–64.
- [Murthy et al. 2008] G. V. S. Murthy, S. Ghosh, M. Das, G. Das, and R. N. Ghosh, “Correlation between ultrasonic velocity and indentation-based mechanical properties with microstructure in Nimonic 263”, *Mater. Sci. Eng. A* **488**:1–2 (2008), 398–405.
- [Murthy et al. 2009] G. V. S. Murthy, G. Sridhar, A. Kumar, and T. Jayakum, “Characterization of intermetallic precipitates in a Nimonic alloy by ultrasonic velocity measurements”, *Mater. Charact.* **60**:3 (2009), 234–239.
- [Palanichamy et al. 1995] P. Palanichamy, A. Joseph, T. Jayakumar, and B. Raj, “Ultrasonic velocity measurements for estimation of grain size in austenitic stainless steel”, *NDT & E Int.* **28**:3 (1995), 179–185.
- [Papadakis 1970] E. P. Papadakis, “Ultrasonic attenuation and velocity in SAE 52100 steel quenched from various temperatures”, *Metall. Trans.* **1**:4 (1970), 1053–1057.
- [Ringer et al. 1997] S. P. Ringer, T. Sakurai, and I. J. Polmear, “Origins of hardening in aged Al-Cu-Mg-(Ag) alloys”, *Acta Mater.* **45**:9 (1997), 3731–3744.
- [Rokhlin and Matikas 1996] S. I. Rokhlin and T. E. Matikas, “Ultrasonic characterization of surfaces and interphases”, *Mater. Res. Soc. Bull.* **21**:10 (1996), 22–29.
- [Rosen et al. 1985] M. Rosen, L. Ives, S. Ridder, F. Biancaniello, and R. Mehrabian, “Correlation between ultrasonic and hardness measurements in aged aluminum alloy 2024”, *Mater. Sci. Eng.* **74**:1 (1985), 1–10.
- [dos Santos Mesquita and Halldórsdóttir 2005] M. dos Santos Mesquita and S. Halldórsdóttir, “Data analysis: filtering, cross-correlation, coherence and applications to geophysical data using Matlab”, 2005, Available at http://www.geophys.uu.se/cj/geofysdatabeh/notes/report_with_matlab.pdf.
- [Vasudevan and Palanichamy 2002] M. Vasudevan and P. Palanichamy, “Characterization of microstructural changes during annealing of cold worked austenitic stainless steel using ultrasonic velocity measurements and correlation with mechanical properties”, *J. Mater. Eng. Perform.* **11**:2 (2002), 169–176.
- [Verhoeven 2005] J. D. Verhoeven, *Metallurgy of steel for bladesmiths & others who heat treat and forge steel*, Iowa State University, Ames, IA, 2005.

Received 27 Jun 2012. Revised 22 Oct 2012. Accepted 30 Oct 2012.

MOHAMMAD HAMIDNIA: m_hamidnia74@yahoo.com

NDE Lab., Faculty of Mechanical Engineering, K. N. Toosi University of Technology, Pardis St., MollaSadra Ave., Vanak Sq., Tehran, Iran

FARHANG HONARVAR: honarvar@mie.utoronto.ca

NDE Lab, Faculty of Mechanical Engineering, K. N. Toosi University of Technology, Pardis St., MollaSadra Ave., Vanak Sq., Tehran, Iran

JOURNAL OF MECHANICS OF MATERIALS AND STRUCTURES

msp.org/jomms

Founded by Charles R. Steele and Marie-Louise Steele

EDITORS

CHARLES R. STEELE	Stanford University, USA
DAVIDE BIGONI	University of Trento, Italy
IWONA JASIUK	University of Illinois at Urbana-Champaign, USA
YASUHIDE SHINDO	Tohoku University, Japan

EDITORIAL BOARD

H. D. BUI	École Polytechnique, France
J. P. CARTER	University of Sydney, Australia
R. M. CHRISTENSEN	Stanford University, USA
G. M. L. GLADWELL	University of Waterloo, Canada
D. H. HODGES	Georgia Institute of Technology, USA
J. HUTCHINSON	Harvard University, USA
C. HWU	National Cheng Kung University, Taiwan
B. L. KARIHALOO	University of Wales, UK
Y. Y. KIM	Seoul National University, Republic of Korea
Z. MROZ	Academy of Science, Poland
D. PAMPLONA	Universidade Católica do Rio de Janeiro, Brazil
M. B. RUBIN	Technion, Haifa, Israel
A. N. SHUPIKOV	Ukrainian Academy of Sciences, Ukraine
T. TARNAI	University Budapest, Hungary
F. Y. M. WAN	University of California, Irvine, USA
P. WRIGGERS	Universität Hannover, Germany
W. YANG	Tsinghua University, China
F. ZIEGLER	Technische Universität Wien, Austria

PRODUCTION production@msp.org

SILVIO LEVY Scientific Editor

See msp.org/jomms for submission guidelines.

JoMMS (ISSN 1559-3959) at Mathematical Sciences Publishers, 798 Evans Hall #6840, c/o University of California, Berkeley, CA 94720-3840, is published in 10 issues a year. The subscription price for 2012 is US \$555/year for the electronic version, and \$735/year (+\$60, if shipping outside the US) for print and electronic. Subscriptions, requests for back issues, and changes of address should be sent to MSP.

JoMMS peer-review and production is managed by EditFLOW® from Mathematical Sciences Publishers.

PUBLISHED BY

 **mathematical sciences publishers**

nonprofit scientific publishing

<http://msp.org/>

© 2012 Mathematical Sciences Publishers

Journal of Mechanics of Materials and Structures

Volume 7, No. 10

December 2012

-
- Indentation and residual stress in the axially symmetric elastoplastic contact problem** TIAN-HU HAO 887
- Form finding of tensegrity structures using finite elements and mathematical programming** KATALIN K. KLINKA, VINICIUS F. ARCARO and DARIO GASPARINI 899
- Experimental and analytical investigation of the behavior of diaphragm-through joints of concrete-filled tubular columns** RONG BIN, CHEN ZHIHUA, ZHANG RUOYU, APOSTOLOS FAFITIS and YANG NAN 909
- Buckling and postbuckling behavior of functionally graded Timoshenko microbeams based on the strain gradient theory** REZA ANSARI, MOSTAFA FAGHIH SHOJAEI, VAHID MOHAMMADI, RAHEB GHOLAMI and MOHAMMAD ALI DARABI 931
- Measurement of elastic properties of AISI 52100 alloy steel by ultrasonic nondestructive methods** MOHAMMAD HAMIDNIA and FARHANG HONARVAR 951
- Boundary integral equation for notch problems in an elastic half-plane based on Green's function method** Y. Z. CHEN 963
- Internal structures and internal variables in solids** JÜRI ENGELBRECHT and ARKADI BEREZOVSKI 983
- The inverse problem of seismic fault determination using part time measurements** HUY DUONG BUI, ANDREI CONSTANTINESCU and HUBERT MAIGRE 997



1559-3959(2012)7:10;1-#